

Subscriber access provided by Basel University Library

Genetically encoded stimuli-responsive cytoprotective hydrogel capsules for single cells provide novel genotype-phenotype linkage

Rosario Vanella, Alfred Bazin, Duy Tien Ta, and Michael A. Nash

Subscriber access provided by Basel University Library

Chem. Mater., **Just Accepted Manuscript** • DOI: 10.1021/acs.chemmater.8b04348 • Publication Date (Web): 09 Jan 2019

Downloaded from <http://pubs.acs.org> on January 17, 2019

Just Accepted

“Just Accepted” manuscripts have been peer-reviewed and accepted for publication. They are posted online prior to technical editing, formatting for publication and author proofing. The American Chemical

Subscriber access provided by Basel University Library

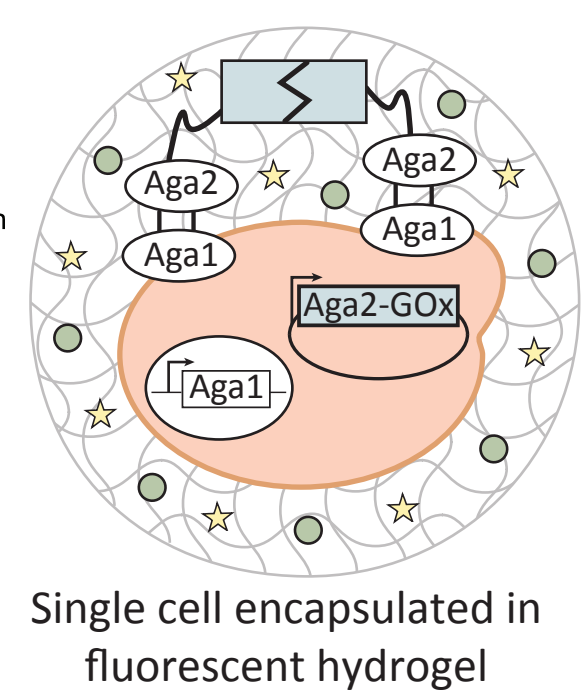
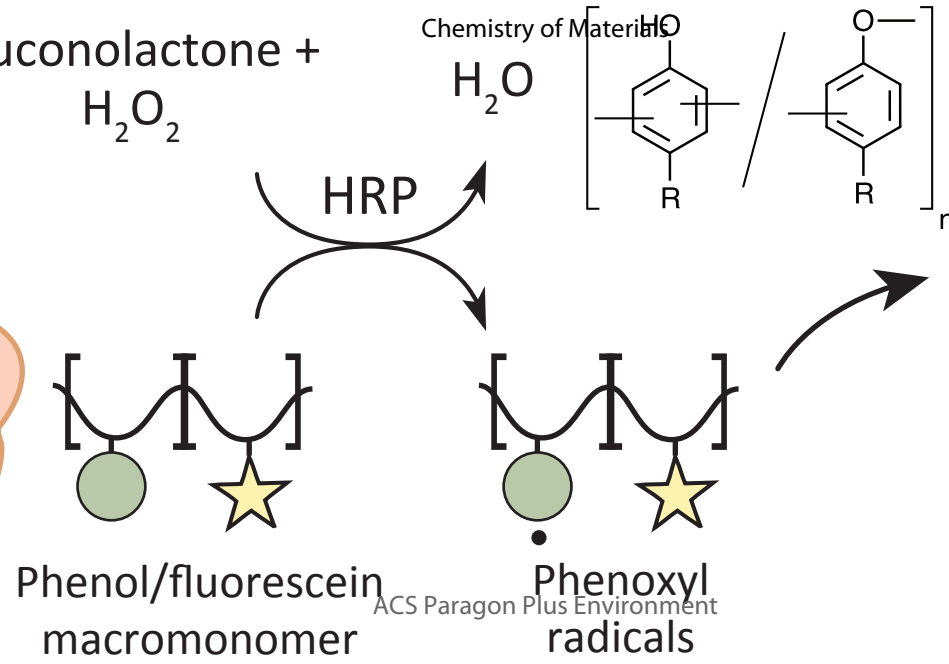
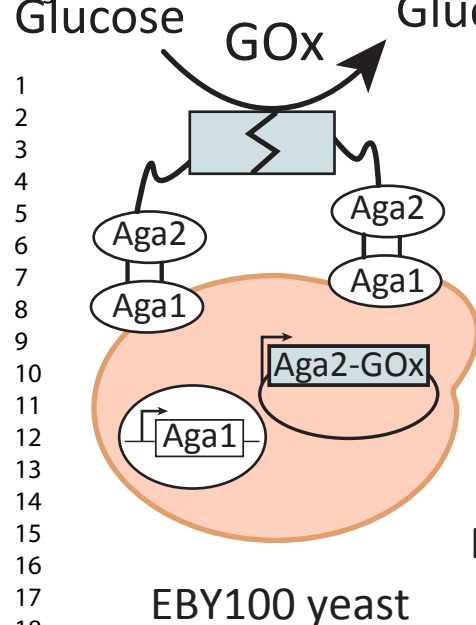
Society provides “Just Accepted” as a service to the research community to expedite the dissemination of scientific material as soon as possible after acceptance. “Just Accepted” manuscripts appear in full in PDF format accompanied by an HTML abstract. “Just Accepted” manuscripts have been fully peer reviewed, but should not be considered the official version of record. They are citable by the

Subscriber access provided by Basel University Library

Digital Object Identifier (DOI®). “Just Accepted” is an optional service offered to authors. Therefore, the “Just Accepted” Web site may not include all articles that will be published in the journal. After a manuscript is technically edited and formatted, it will be removed from the “Just Accepted” Web site and published as an ASAP article. Note that technical editing may introduce minor changes

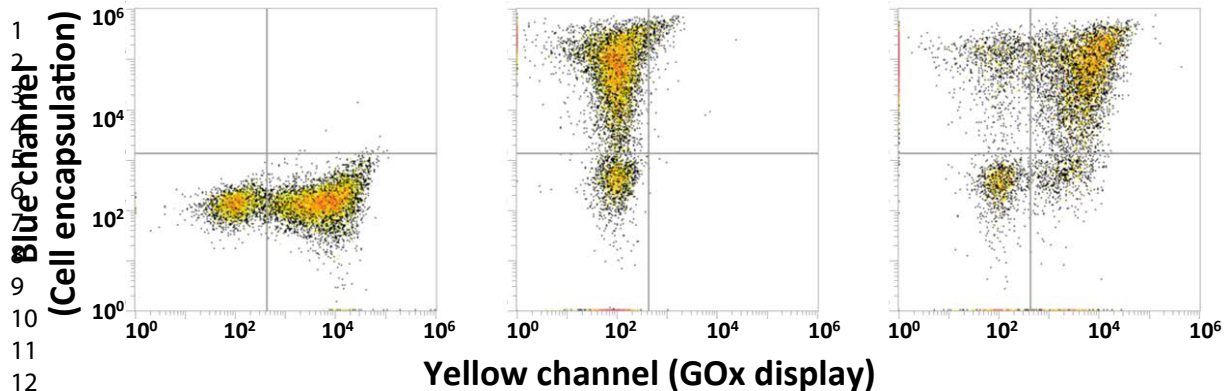
Subscriber access provided by Basel University Library

to the manuscript text and/or graphics which could affect content, and all legal disclaimers and ethical guidelines that apply to the journal pertain. ACS cannot be held responsible for errors or consequences arising from the use of information contained in these “Just Accepted” manuscripts.



A

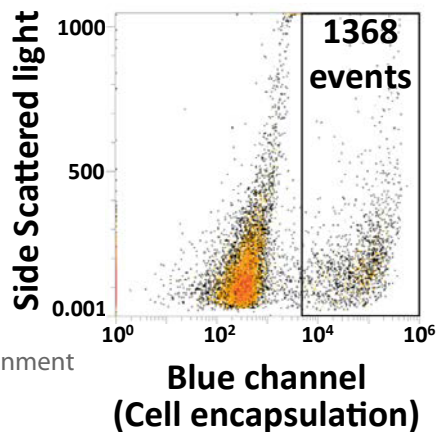
(i) WT GOx display

Chemical synthesis of materials
(ii) WT GOx encapsulationPage 23 of 23
(iii) WT GOx display & encapsulation

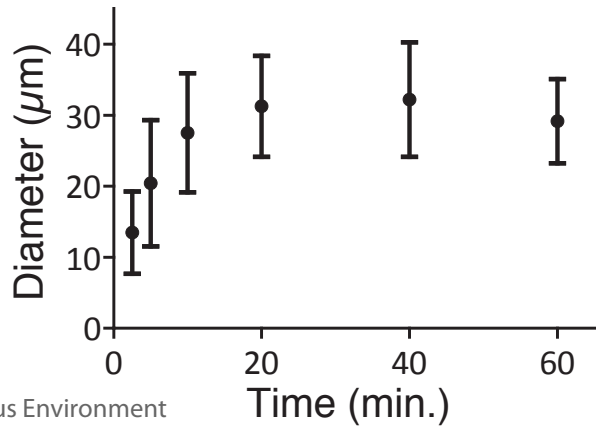
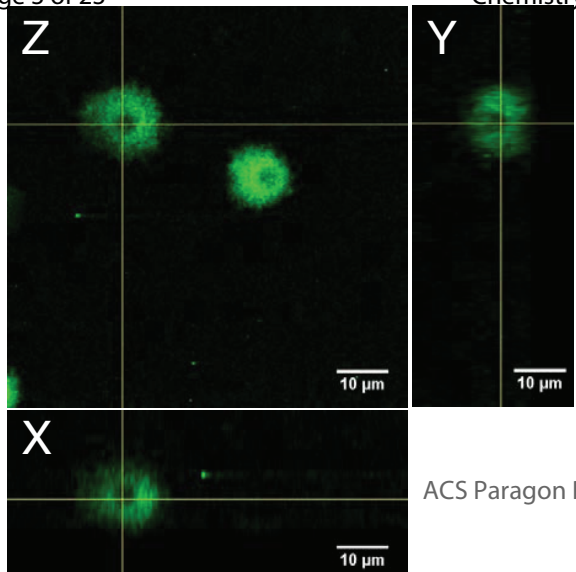
B

Yeast mixture (% GOx-positive cells)	# of encapsulated cells out of 10'000
100%	5923
75%	3980
50%	2890
25%	1368
10%	463
1%	65
0%	15

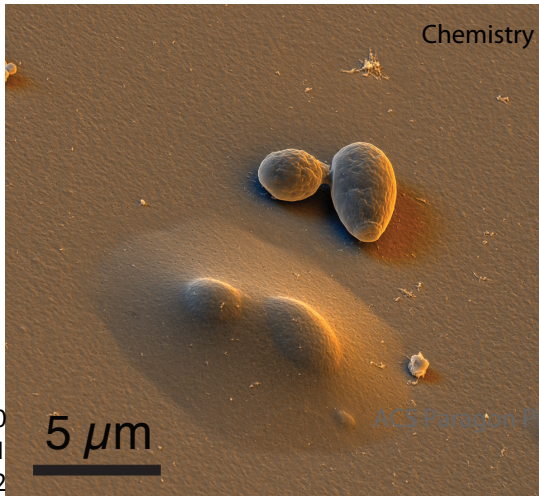
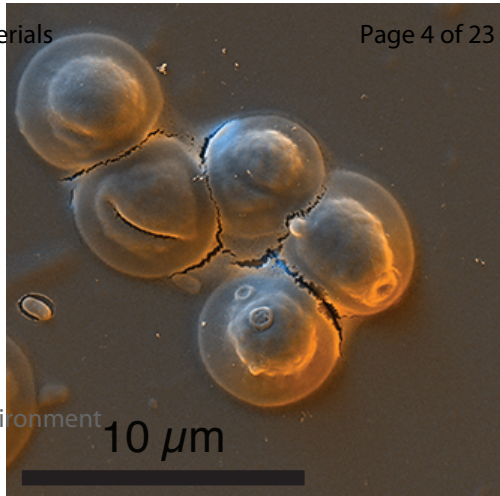
25% GOx wild type cells

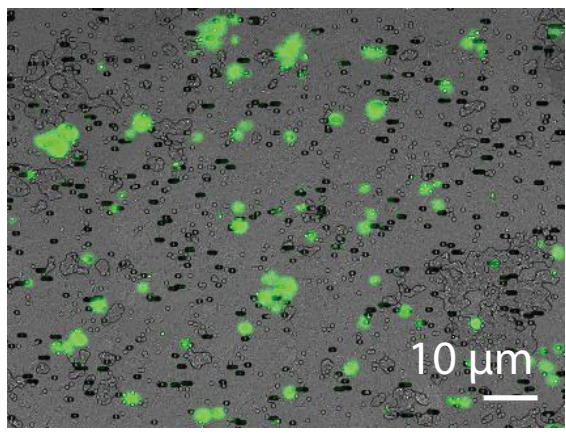
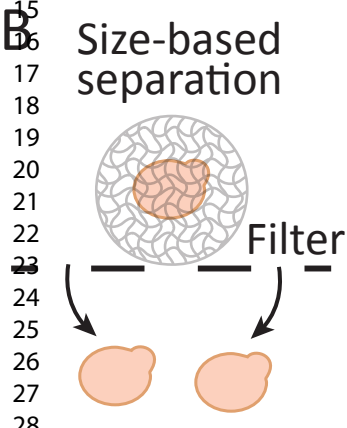
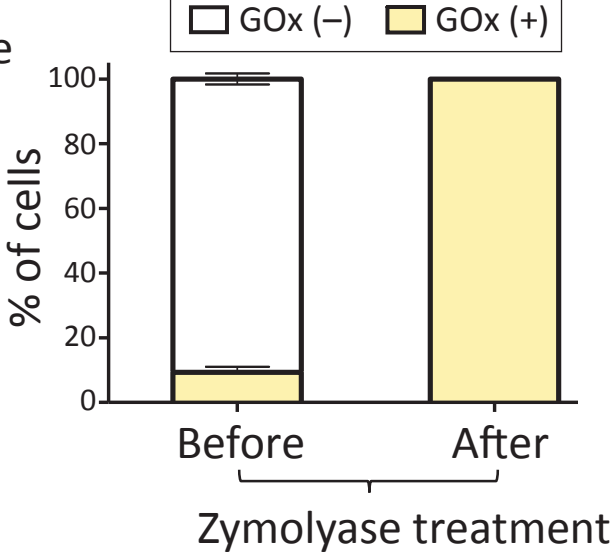
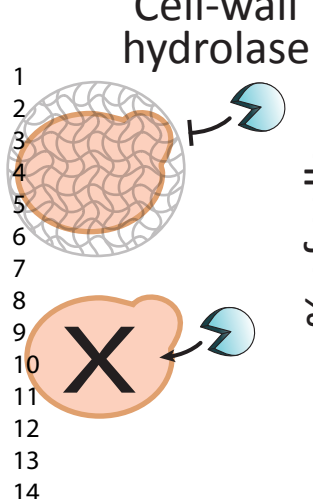


1
2
3
4
5
6
7
8
9
10
11
12
13
14
15
16

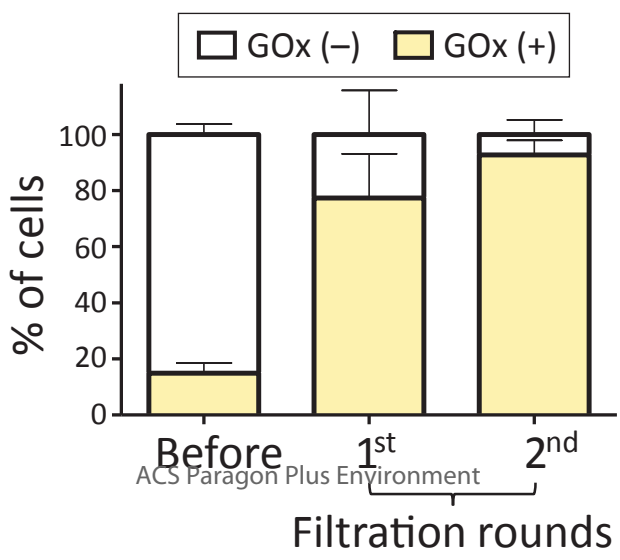


ACS Paragon Plus Environment

A1
2
3
4
5
6
7
8
9
10
11
12
13**B**



Encapsulated cells are captured by filter



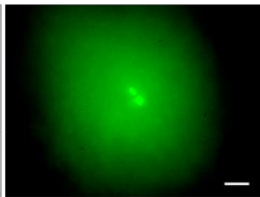
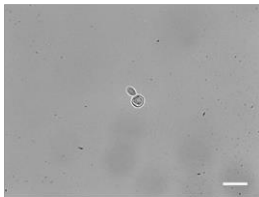
A

Bright field

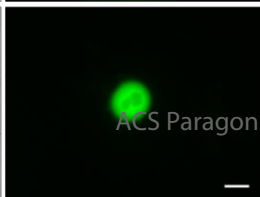
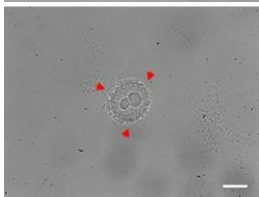
Fluorescence

1
2
3
4
5
6
7
8
9
10
11
12

pH 6

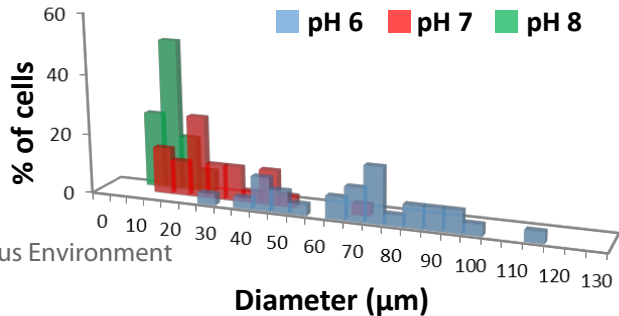


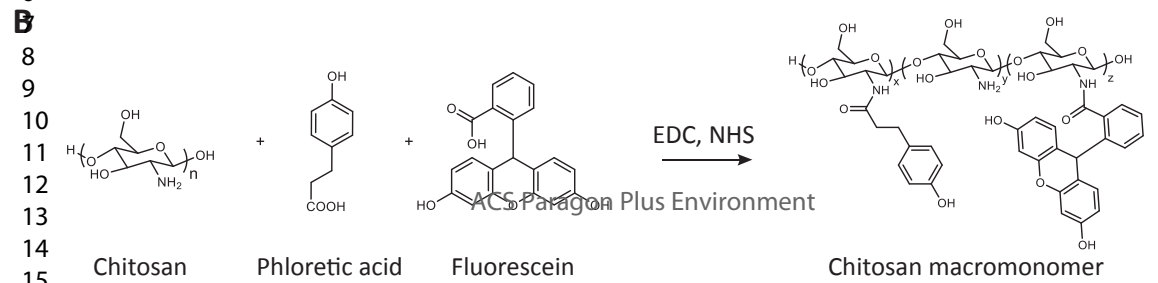
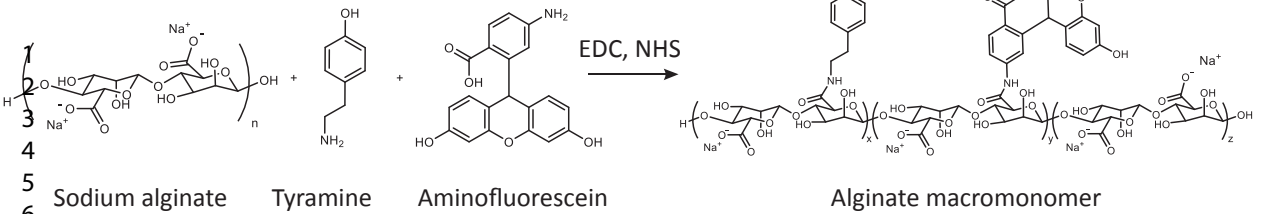
pH 8



ACS Paragon Plus Environment

B





Genetically encoded stimuli-responsive cytoprotective hydrogel capsules for single cells provide novel genotype-phenotype linkage

Rosario Vanella^{1,2}, Alfred Bazin^{1,2,3}, Duy Tien Ta^{1,2}, and Michael A. Nash^{1,2*}

¹ Department of Chemistry, University of Basel, 4058 Basel, Switzerland.

² Department of Biosystems Science and Engineering, ETH Zurich, 4058 Basel, Switzerland.

³ European School of Chemistry, Polymers and Materials, University of Strasbourg, 67087 Strasbourg, France.

*Correspondence to michael.nash@unibas.ch

Abstract

Modification of cell surfaces with synthetic polymers is a promising approach for regulating cellular behavior. Here we describe a genetically controlled strategy for selectively encapsulating single yeast cells in synthetic microniches comprised of cross-linked phenol-modified alginate and chitosan hydrogel capsules. Our system links inducible gene expression with enzyme-mediated hydrogel polymerization and provides a novel genotype-phenotype linkage whereby only cells carrying a requisite gene encoding a flavin adenine dinucleotide (FAD)-dependent oxidoreductase undergo autonomous enzyme-mediated surface polymerization resulting in formation of hydrogel capsules. The composition of the hydrogel capsules is highly tunable and the capsule sizes are pH-responsive, allowing for control of capsule porosity and shell diameters over a range of 15-80 μm . The hydrogel capsules prevent extracellular proteins from reaching the cell surface, thereby conferring cellular immunity to lytic enzyme cocktails and rendering the hydrogel capsules cytoprotective against osmotic shock. We demonstrate the utility of this genetically controlled artificial hydrogel-encapsulated cell phenotype by isolating and enriching uniform eukaryotic cell lineages from genetically heterogeneous cell mixtures at 95-100% efficiency. The encapsulated cells remained viable and were capable of dividing and breaking free from their hydrogel capsules, allowing further propagation of selected cells. Our bottom-up approach to cellular compartmentalization links inducible intracellular genetic components with an artificial extracellular matrix that resists enzymatic lysis and mediates communication with the surrounding environment through a size-tunable and permeable hydrogel capsule.

Introduction

Compartmentalization is a defining feature of living systems. Cells, tissues and organs all exhibit an extraordinary degree of spatial segregation in form and function which is necessary for carrying out the daily activities of life. In an effort to advance synthetic biological systems, research has focused on developing compartmentalization strategies that function at the molecular-to-cellular length scales¹⁻⁶. Specifically, encapsulation of individual cells inside synthetic conformal hydrogels⁷⁻⁹ has attracted significant attention. The ability of conformal synthetic hydrogels to serve as optical labels, act as steric protective layers, and separate distinct cell types make these systems potentially useful for rare cell isolation and *in vivo* cellular therapies^{10,11}.

Several early demonstrations of cellular encapsulation technology utilized formation of multicellular aggregates on the scale of 0.1-1 mm by relying on self-assembly of oppositely charged polyelectrolyte chains^{12,13} or incorporation of cells in agarose emulsions¹⁴. Polymerization-based approaches have further been developed which rely on cross-linking polymer materials from monomeric precursor solutions¹⁵⁻²¹. Photoinitiators have also been conjugated to biomolecules (e.g., antibodies)²² which specifically recognize target cells and generate free radicals upon light exposure. In such systems, target cells within a heterogeneous mixture can be selectively encapsulated by photo-initiated polymerization in the presence of monomers.

Enzymatic initiation systems for cellular encapsulation have also been demonstrated in several formats. For example, peroxidase-mediated dityrosine cross-coupling has been used to form hydrogels capsules around cells²³⁻²⁵. Sakai, Taya and co-workers demonstrated single-cell encapsulation based on horseradish peroxidase (HRP)-mediated polymerization, as well as cascade reactions involving glucose oxidase (GOx) as a source of H₂O₂ to feed HRP-mediated reactions^{18,26,27}. Inspired by this prior work, we sought here to utilize the GOx/HRP cascade for cross-linking hydrogels, but instead of supplying the enzymes to cells from the outside, we sought to develop a system in which the polymerization enzyme itself was genetically encoded in DNA plasmids carried by the cells. Gene induction and expression inside the cells then resulted in protein synthesis of the enzymatic initiators. Using secretion and display pathways in yeast, the initiator enzymes were then displayed on the outer cell wall and able to trigger enzymatic cross-linking of hydrogels shells resulting in cell encapsulation. These new innovations rely on the presence or absence of a single copy of a gene inside the cell to produce single-cell hydrogel capsules which serve as an artificial phenotype linked with the genotype of the cells. Our approach which relies on synthesis of enzymatic initiators inside the cells is referred to as ‘bottom-up’ encapsulation, and can be contrasted with the prior systems in which cells were extrinsically labelled with initiator compounds that triggered polymerization/encapsulation reactions, which we refer to as ‘top-down’ encapsulation systems²⁸⁻³¹. An additional level of novelty in the current work is the first demonstration of chitosan capsules for single-cell

1
2
3 encapsulation *via* an enzyme-mediated process, which is significant because the chitosan shells are size
4 tunable depending on the pH of the surrounding media.
5
6

7 Pitzler et al³² also demonstrated a bottom-up polymerization system where expression of glucose
8 phosphatase was coupled with Fenton chemistry to produce hydrogels at the *E. coli* surface, however in that
9 prior work the hydrogel served as a fluorescent tag and was not shown to be uniform, robust or sufficiently
10 thick to confer altered physical properties to cells that could be used for large scale selections. Our hydrogels
11 in contrast form uniform capsules, are physically robust, tens of microns thick, and capable of protecting
12 cells from osmotic lysis. The shells shown here further impart new physico-chemical properties such as
13 significantly increased cell size and pH-responsiveness that enable new cell isolation procedures (e.g., size-
14 based filtration) that are useful for various synthetic biology applications. Our strategy therefore represents
15 the first cell encapsulation system that utilizes inducible genes to create well-defined cytoprotective hydrogel
16 enclosures around live eukaryotic cells. Such an approach has significant potential in cell screening, cell-
17 based therapy and directed evolution applications where the cytoprotection and/or isolation of specific cell
18 genotypes are of high interest.
19
20
21
22
23
24
25

26 27 **Experimental Section**

28
29 **Materials.** All the chemicals used in this work were purchased from Sigma Aldrich if not otherwise
30 specified. The primary and secondary antibody were purchased from Thermo Fisher Scientific. Restriction
31 enzymes were bought from New England Biolabs. Sodium Alginate (Viscosity 1%: 100 - 200 mPa.s) was
32 purchased from Duchefa Biochemie. Zymolyase 100T was purchased from Roth.
33
34
35
36

37 **Preparation of fluorescent alginate and chitosan with phenol groups.** Alginate and chitosan with phenol
38 moieties and fluorescein were prepared through carbodiimide activation chemistry³³. Sodium alginate (avg.
39 M_w 70,000 Da) was dissolved in 50 mM MES buffer pH 6 at a final concentration of 10 mg/mL. After the
40 alginate was completely dissolved, tyramine hydrochloride, NHS and EDC were added to the sodium
41 alginate solution at 7, 1.2,3.9 mg/mL respectively. Finally, 6-aminofluorescein was added to a final
42 concentration of 0.25 mg/mL. Chitosan (avg. M_w 50,000-190,000 Da) was dissolved in a pH 2 solution of
43 HCl at a final concentration of 10 mg/mL. After the chitosan was completely dissolved, the pH was raised to
44 4.5 by adding NaOH. Then phloretic acid, NHS and EDC were added to the chitosan solution at 7, 1.2,3.9
45 mg/mL respectively. Finally, fluorescein was added to a final concentration of 0.25 mg/mL. Both the
46 reactions were incubated at room temperature for 16 to 20 hours with vigorous stirring and then precipitated
47 dropwise into 80% ethanol aqueous solutions. The alginate was then washed with 80% ethanol and the final
48 product dissolved in water before being lyophilized. Chitosan was then washed with 80% ethanol and then
49 acetone. The final product was dissolved in an acidic solution at pH 2. After dissolution of the modified
50 chitosan, the pH was raised to 5 by adding NaOH before being lyophilized. The success of the conjugations
51 was confirmed through ¹H-NMR (**Figure S1**).
52
53
54
55
56
57
58
59
60

1
2
3 **Amplification and cloning of the Wild-type GOx gene.** The GOx wild type gene was amplified from the
4 genome of *Aspergillus niger* strain 4247 (LGC Standards) using the primers F1 (5'-
5 GCATACGGATCCATGCAGACTCTCCTTGTGAGCTCGC-3') and R1 (5'-
6 GCATACCTCGAGTCACTGCATGGAAGCATAATCTTCC-3'), and cloned using *Bam*HI and *Xho*I
7 restriction sites into the yeast plasmid pYD1 for protein display (gift from Dane Wittrup, Addgene plasmid
8 #73447)³⁴. After sequence confirmation, the plasmid pYD1-GOx was transformed into *Saccharomyces*
9 *cerevisiae* EBY100 following a typical lithium acetate transformation³⁵ procedure and selecting the positive
10 colonies on SD agar 2% (w/v) glucose plates lacking tryptophan (-Trp). Resulting colonies were cultivated in
11 liquid SD -TRP liquid medium with 2% glucose for 24 hours at 30°C with continuous shaking at 200 rpm.
12 Protein expression and display was then induced by transferring the culture to a fresh liquid medium lacking
13 tryptophan containing 0.2% (w/v) glucose and 1.8% (w/v) galactose, and shaking for 24 hours at 30°C.

21 **Amplex Red enzymatic assay.** Yeast cells displaying Glucose Oxidase (GOx) were used to perform an
22 Amplex Red enzymatic assay in order to test for the functionality of the expressed enzyme. The reaction
23 mixture consisted of $\sim 10^6$ yeast cells, 100 mM Glucose, 4.5 μ M HRP and 10 μ M Amplex Red in 50mM of
24 Phosphate Buffer (pH 7.4). The fluorescence was read at 590 nm every 1 min for 10 min (Figure S2).

28 **GOx antibody labelling.** The expression and display of GOx was confirmed by antibody labelling. $\sim 2 \times 10^6$
29 induced yeast cells were washed with 1 mL PBS containing 0.1% BSA and then resuspended and incubated
30 at room temperature for 30 min with 1/200 dilution of the primary anti-Xpress antibody (stock concentration
31 of 1.2 mg/mL). After incubation, the cells were washed with 1 mL of ice-cold PBS + 0.1% BSA and then
32 resuspended in ice cold buffer containing 1/200 dilution of the goat anti mouse IgG secondary antibody
33 (stock concentration 2 mg/mL) conjugated with Alexa Fluor 555. After 20 min incubation on ice, the cells
34 were pelleted, washed with cold buffer and resuspended just before flow cytometry. As a negative control,
35 the same yeast cells carrying the plasmid pYD1-GOx wild type were treated only with the secondary
36 antibody conjugated with Alexa Fluor 555.

43 **Cell encapsulation in fluorescent alginate and chitosan.** After induction of protein expression, yeast cells
44 displaying GOx were washed with 50 mM sodium phosphate buffer pH 7.4 and resuspended in the same
45 buffer at a final OD₆₀₀ of 0.2. Glucose, HRP and the modified alginate were added to the cell sample at final
46 concentrations of 100 mM, 4.5 μ M, and 0.125% (w/v), respectively. The reaction was gently mixed and
47 incubated at room temperature. After 10 min, four volumes of 50 mM sodium phosphate buffer pH 7.4 were
48 added and the samples were analyzed through flow cytometry or used for single cell sorting. Cell
49 encapsulation in chitosan was performed at the exactly same conditions as for the alginate but replacing the
50 sodium phosphate buffer (pH 7.4) with 50 mM MES buffer at pH 6. When used, mCherry was added to the
51 encapsulation reaction mixture at a final concentration of 4.5 μ M. SEM imaging was performed by first
52 adhering the cells to a coverglass coated with concanavalin, followed by exposure of the coverglass to
53 hydrogel reagents for 10 minutes. Encapsulated cell samples adhered to the coverglass were then fixed in
54
55
56
57
58
59
60

1
2
3 glutaraldehyde dried with acetone, and covered with an evaporated thin gold layer prior to SEM imaging
4 using an FEI Versa3D microscope.
5
6

7 **Flow cytometry, FACS and downstream analysis.** All the single and double stained yeast cells were
8 analyzed with the Attune NxT (Thermo Fisher Scientific) flow cytometer equipped with a 488 nm and a 561
9 nm laser. Yeast cells were sorted using a MoFlo XDP cell sorter from Beckman Coulter equipped with 488
10 nm and 561 nm lasers, and with a 100 μm nozzle. Prior to encapsulation and sorting, the yeast cells were
11 washed and stained with Propidium Iodide (final concentration of 4 $\mu\text{g}/\text{mL}$). The cells positive for the
12 encapsulation reaction and negative for the staining with Propidium Iodide were sorted in single cell mode.
13
14
15

16
17 **Genotype enrichment by cytoprotection against enzymatic lysis.** A mixture of yeast cells containing less
18 than 10% pGAL-GOx genotype positive cells mixed together with 90% cells carrying an empty pYD1
19 plasmid was used to perform a standard cell encapsulation reaction in fluorescent alginate. After cell
20 encapsulation, Zymolyase was added to the reaction mix to a final concentration of 300 U/ml together with 1
21 mM Dithiothreitol (DTT). The reaction was incubated at 35°C with shaking at 1000 rpm for 60 minutes. The
22 cells were then transferred to a -Trp glucose liquid medium and grown for 40 hours before being used for
23 single cell sorting onto -Trp agar plates containing 2% Galactose. After 48 hours, colonies derived from
24 single cell sorted events were assayed for the expression of GOx through an ABTS top agar assay. Glucose
25 (333 mM), ABTS (7 mM) and HRP (2U/ml) were mixed with 2% agar solution and poured on the plate
26 containing the sorted colonies. After 2 to 5 minutes, green halos started to appear above the colonies
27 expressing and displaying the GOx on the cell wall. As a negative control the same yeast population was
28 processed in parallel but without treatment with the lytic enzymes mixture.
29
30
31
32
33
34
35

36
37 **Genotype enrichment by size-based filtration.** A yeast population containing less than 10% pGAL-Gox
38 genotypic positive cells was used to perform a standard cell encapsulation reaction in fluorescent alginate.
39 After encapsulation the sample was filtered through polycarbonate membranes with 10 μm pores sizes
40 (Whatman) by applying vacuum. Afterwards the membrane was washed three times with 50 mM sodium
41 phosphate buffer at pH 7.4. Finally the encapsulated cells retained by the filter were recovered by rinsing the
42 the membrane with sodium phosphate buffer (pH 7.4) and analyzed with flow cytometry.
43
44
45
46

47 **pH-responsive chitosan capsules.** Multiple samples of yeast cells displaying GOx were washed with 50
48 mM MES buffer pH 6 and resuspended in the same buffer at a final OD_{600} of 0.2. Glucose, HRP and the
49 fluorescent modified chitosan were added to the cells at final concentrations of 100 mM, 4.5 μM , and
50 0.125% (w/v), respectively. The reactions were gently mixed and incubated at room temperature. After 20
51 min, different samples were diluted respectively with four volumes of 50 mM MES buffer pH 6, 50 mM
52 phosphate buffer pH 7.4 or 50 mM phosphate buffer pH 8.2 to stop the encapsulation reaction. The pH of
53 each sample was measured and if needed corrected to final pH values of 6, 7 or 8. The size of the capsules at
54 each pH was analysed through microscopy by measuring the diameter of multiple randomly picked cell-
55 hydrogel units ($n > 25$ for each pH value).
56
57
58
59
60

Results and Discussion

Our reaction system relies on an enzymatic cascade involving glucose oxidase (GOx) and horseradish peroxidase (HRP) to cross-link phenol groups grafted onto various macromonomer species. GOx is a highly glycosylated homodimeric flavoprotein, 160 kDa in size that catalyzes the oxidation of β -D-glucose to D-gluconolactone and hydrogen peroxide using molecular oxygen as an electron acceptor³⁶. Recently we demonstrated the use of GOx in combination with Fenton's reagent for quantifying enzyme activity based on fluorescent hydrogel formation^{37,38}. In the current system, GOx and HRP worked in tandem as a bi-enzymatic initiation system for polymerization of phenolated macromonomers³⁹⁻⁴².

To synthesize enzyme-crosslinkable species, macromonomers of alginate and chitosan were modified with phenol and fluorescein groups using carbodiimide activation chemistry. Sodium alginate was conjugated with tyramine and aminofluorescein^{33,43} (**Scheme 1A**), and chitosan was coupled with fluorescein and phloretic acid^{44,45} (**Scheme 1B**). Following extensive washing and lyophilization, the presence of the aromatic groups of phenol and fluorescein moieties was confirmed using proton nuclear magnetic resonance (¹H-NMR) spectroscopy (**Figure S1**). We tested the ability of the GOx/HRP cascade to cross-link phenolated monomers in free solution (i.e., without cells) by combining 10 mg/mL of modified alginate or chitosan macromonomers with 0.5 μ M GOx and 4.5 μ M HRP in sodium phosphate buffer (pH 7.4). Upon addition of 100 mM D-glucose, the solution rapidly gelled within a few seconds. Negative controls lacking the HRP or GOx remained liquid. These observations confirmed that the modified macromonomers could be rapidly cross-linked through the GOx/HRP cascade.

We sought to adapt the enzyme-mediated polymerization system to modify, visualize, and isolate cells containing specific genes amidst genetically heterogeneous cell populations based purely on physical properties of the hydrogel capsules. In order to connect the hydrogel polymerization with the genotype of a specific cell line, we incorporated GOx into a eukaryotic cellular display system, and tested the ability of cells carrying the GOx gene to auto-encapsulate in hydrogel shells. HRP, phenolated fluorescent macromonomers, and glucose were presented in the medium to GOx-displaying cells (**Figure 1**) to initiate the encapsulation reaction. To express GOx on the cell wall, a gene encoding *Aspergillus niger* GOx was cloned in frame with the yeast a-agglutinin subunit 2 (Aga2p)⁴⁶ to create an artificial protein display construct.

Translocation and anchoring of Aga2p-GOx to a-agglutinin subunit 1 (Aga1p) on the cell wall were verified by immunostaining with Alexa Fluor 555-conjugated antibodies against a protein tag located between Aga2p and GOx in the fusion construct. Using analytical flow cytometry, we observed an increase in fluorescence for a major fraction of the cell population (~ 60%), indicating successful display of the enzyme (**Figure 2A, i**). The activity of the displayed enzyme was tested using a coupled HRP/Amplex red assay, which confirmed GOx activity and therefore successful homodimerization of GOx on the cell wall (**Figure S2**).

1
2
3 Cells displaying functional GOx homodimers were next used to develop the cell encapsulation
4 system. 2×10^6 yeast cells/mL displaying GOx were suspended in a solution of 100 mM glucose, 4.5 μ M
5 HRP, and 0.125% (w/v) of phenolated alginate. After 10 min. reaction at room temperature, the samples
6 were analyzed and a significant percentage (~60%) of cells corresponding to the same percentage
7 successfully stained for GOx exhibited strong green fluorescence derived from fluorescein, consistent with
8 the formation of fluorescent hydrogel shells around the cells (**Figure 2A, ii**). We further tested the
9 encapsulation procedure with a yeast population displaying GOx that had previously been stained with Alexa
10 Fluor 555 for the display of GOx on the cell wall. As shown in **Figure 2A, iii**, after incubation in the reaction
11 mixture a majority of the cell population prestained with red fluorescent antibodies targeting GOx also
12 gained green fluorescence signal due to the formation of the fluorescent hydrogel. This result confirmed that
13 cells expressing GOx were the same cells in the mixture capable of auto-encapsulating in fluorescent
14 hydrogels.
15
16
17
18
19
20
21
22

23 To further prove the specificity of the cellular encapsulation system, we tested the encapsulation
24 procedure using different cell reference mixtures containing diluted amounts of GOx-positive cells at a fixed
25 total number of cells. After encapsulation, the flow cytometry plots showed a precise correspondence
26 between the percentage of GOx positive cells present in the cell mixtures and the number of fluorescein
27 stained cells detected after encapsulation (**Figure 2B**). Moreover, 25 gated cells sorted in single cell mode
28 from a mixture containing 10% GOx positive events were re-cultured and singularly tested for GOx activity.
29 All of them tested positive for functional GOx, indicating the fidelity of the encapsulation process despite the
30 presence of a limited number of positive events in the starting sample (**Figure S3**).
31
32
33
34
35

36 We characterized the morphology of the alginate hydrogel capsules using confocal fluorescence
37 microscopy. A well-defined conformal fluorescent alginate hydrogel was observed surrounding the cells
38 (**Figure 3A**). The orthogonal views show a homogenous distribution of hydrogel surrounding the dark cell
39 mass in the center. A 3D spatial representation is presented in **Figure S4**. We confirmed that only single
40 cells and not clusters of multiple cells were being encapsulated using widefield and confocal fluorescence
41 microscopy on a large number of encapsulated cell populations obtained through multiple independent
42 experiments. We consistently observed dark spots (single cells) or budding yeast inside the green fluorescent
43 capsules (**Figure S5**). The single cell nature of the encapsulation reaction was also confirmed using
44 analytical flow cytometry plots of the scattered pulse height vs. scattered pulse width per event, which
45 distinguished between single cells, budding yeast cells, and cell aggregates (**Figure S6**).
46
47
48
49
50
51
52

53 We investigated the kinetics of gel formation by measuring the thickness of the hydrogel shells using
54 fluorescence microscopy and image analysis following incubation of the reaction for various lengths of time.
55 **Figure 3B** shows that the alginate shells grew rapidly during the first few minutes, reaching a particle
56 diameter of $\sim 30 \mu$ m including the entrapped cell. This rapid growth was followed by a plateau phase wherein
57 extended incubation times (>10 min) did not increase the size of the hydrogel shells. This is an advantageous
58 feature of the system that we attribute to auto-inhibition of the reaction. Auto-inhibition is expected upon
59
60

1
2
3 formation of the alginate shell which provides a diffusion barrier that prevents new macromonomers from
4 reaching the GOx/HRP enzymes at the cell surface. In this case, the reaction will only promote the formation
5 of radical species in the proximity of the cell surface. The extremely short half life of the radical species ⁴⁷
6 does not allow the free radicals to encounter and react with unpolymerized monomers after the hydrogel
7 reaches a critical thickness. Scanning electron microscopy (SEM) (**Figure 4A & B**) was further used to
8 visualize the cells, and confirmed the presence of singly encapsulated uniformly coated yeast cells. Due to
9 the vacuum conditions, the hydrogel capsules appeared slightly smaller on the SEM images than in the
10 confocal fluorescence images.
11
12
13
14
15

16 We tested whether the hydrogel shells could entrap proteins present in the medium and serve as a
17 diffusion barrier for macromonomers and proteins. The cell encapsulation experiment was performed in the
18 presence of mCherry, a ~29 kDa fluorescent protein. The results showed that mCherry was trapped and held
19 within the gel network (**Figure S7**) over several hours. We expect that HRP and macromonomers, with their
20 higher molecular weight of ~44 kDa and ~70 kDa respectively, are similarly limited in their diffusion by the
21 forming gel. We note that in the kinetic growth experiments, it is not possible that the growth plateau is due
22 to consumption of the substrate since the reaction is performed at saturating concentrations of glucose, HRP
23 and macromonomer species. We tested the cytocompatibility of the alginate shells by measuring growth
24 curves of yeast alone, in the presence of the reaction mixture but lacking HRP, and encapsulated in the
25 hydrogel capsules. All three of these growth curves were found to be the same (**Figure S8**), demonstrating
26 that the hydrogel capsules did not inhibit cell growth. The cells are able to grow and divide inside the
27 capsules until they eventually break free from the alginate hydrogel capsules. **Supplementary Movie 1**
28 shows a single budding yeast cell growing and dividing inside the alginate capsule over the course of 15
29 hours.
30
31
32
33
34
35
36
37
38

39 The artificial alginate layer formed around cells displaying functional GOx also served as an
40 enhanced safeguard against cytotoxic agents. The cytoprotective function of the alginate shell was tested
41 through incubation of a heterogeneous population of yeasts containing less than 10% of GOx positive
42 encapsulated cells with Zymolyase, which is a mixture of lytic enzymes that digests the yeast cell wall
43 leading to osmotic lysis and cell death. After incubation with 300 U/ml of Zymolyase for 60 minutes, the cell
44 mixture containing 10% GOX-positive cells was recultivated and sorted in single cell mode onto agar plates.
45 The clonal colonies were then assayed for GOx activity and the fraction of GOx-positive colonies was found
46 to be 100%. This result indicated that the hydrogel capsules conferred resistance to enzymatic lysis to GOx-
47 positive cells (**Figure 5A**) with zero background level survival. Although the hydrogel capsule is porous and
48 allows the diffusion of small nutrients and molecules, it acts as diffusion barrier for large macromolecules
49 such as proteins and enzymes and therefore inhibited Zymolyase enzymes from attaching to and digesting
50 the cell wall. The porosity of the alginate gel layer and as a consequence the efficacy of the diffusion barrier
51 can be tuned by varying the concentration of crosslinkable moieties in the conjugation reaction.
52
53
54
55
56
57
58
59
60

1
2
3 The alginate layer formed around the cells carrying the pGAL-GOx genes provided new physical
4 properties to the cells, a feature we refer to as an artificial phenotype. We exploited the significant increase
5 in apparent cell size that occurs upon enzymatic encapsulation in a filtration process to separate encapsulated
6 cells from non-encapsulated cells (**Figure 5B**). Heterogeneous populations of yeast cells where 10% of cells
7 carried the pGAL-GOx gene were first encapsulated in fluorescent alginate and then filtered through 10 μm
8 pores size filters. As expected, the bare yeast cells (2 to 5 μm in diameter) could easily pass through the filter
9 and were discarded in the flow through. Encapsulated yeast cells (20 to 30 μm in diameter), however, were
10 retained on the filter and could be recovered for further analysis. **Figure 5B** shows a micrograph of green
11 fluorescent hydrogel capsules adhered onto the polycarbonate filter membrane. The dark spots in the image
12 are the membrane pores. Following this filtration procedure, the yeast cell population encapsulated in
13 fluorescent hydrogel and positive for the pGAL-GOx gene was enriched from 10% to 95% within two
14 filtration steps, each requiring only 2 minutes of processing time (**Figure 5C**). Both the cell survival and
15 filtration procedures have relevant applications for the enrichment of genetic libraries in directed evolution
16 experiments, or in automated genomics applications where a specific genetically tagged cell line can be
17 separated from genetically diverse mixtures, thus providing a rapid, high-throughput, scalable and affordable
18 alternative to cell sorting.

19
20
21 As an alternative to alginate, we further investigated the use of the polysaccharide chitosan for
22 encapsulation of cells. Chitosan has been used in biomedical applications and drug delivery systems due to
23 its biocompatibility and its mechanical and chemical properties⁴⁸. Dissolution of chitosan in aqueous buffers
24 is achieved only at acidic $\text{pH} \leq 6$, when the amino groups of the polymer are protonated. This solubility
25 switch in aqueous environments causes the swelling and deswelling of the polymer based on the pH ⁴⁹. The
26 pH sensitivity of chitosan hydration presented an interesting feature for cell encapsulation applications by
27 providing a tool to tune the permeability and elasticity of the polymer and regulate the accessibility to the
28 encapsulated cells. Chitosan with phenol and fluorescein moieties (**Scheme 1B**) was used for cell
29 encapsulation using a slightly modified protocol at pH 6. Phenolated chitosan showed similar behavior to the
30 modified alginate, however, the chitosan shells showed higher stability and less tendency to form non-
31 specific interactions with filter membranes as compared to alginate. Chitosan capsules were found to be less
32 prone to aggregation and the gel capsules did not break under mechanical stress such as during centrifugation
33 and filtration.

34
35
36 The pH sensitivity of the chitosan capsules was investigated by varying the pH of the solution
37 containing encapsulated cells from 6 to 8 and observing the behavior of the hydrogel capsules using
38 fluorescence microscopy. We note that yeast cells are stable and remain viable in a pH range of 6 to 8,
39 therefore tuning the capsules diameter with pH is compatible with *in vivo* processing and propagation of the
40 cells⁵⁰. Yeast cells encapsulated with fluorescent chitosan at pH 6 presented a well-defined and water
41 swollen shell that was not visible in bright field mode but was clearly visible in fluorescence mode (**Fig 6A**
42 **upper panels**). The chitosan capsule was not visible at pH 6 using bright field imaging because the

1
2
3 refractive index difference between the hydrogel and the surrounding water was too low, and the swollen
4 hydrogel did not scatter sufficient light. Nonetheless, at pH 6, a diffuse bright water-swollen hydrogel was
5 clearly observable using fluorescence imaging (Figure 6A, upper right panel). By resuspending the same cell
6 sample in basic buffer (pH 8), we observed a radical reduction in the size of the gel layer around the cells. At
7 pH 8, the chitosan capsules were clearly visible in both bright field and fluorescence modes (**Figure 6A**
8 **lower panels**). The insolubility of the chitosan at pH 8 triggered dehydration and collapse of the capsule onto
9 the yeast cell. The pH-tunable solubility of the chitosan is based on protonation/deprotonation of the amino
10 groups which have a pKa of ~ 6.5 . This mechanism allowed for visualization of the chitosan hydrogel layer
11 surrounding the cells even bright field mode (Figure 6A, bottom left panel), eliminating the requirement of
12 fluorescence microscopy to visualize the capsules. The fluorescence imaging at pH 8 also indicated a highly
13 condensed hydrogel with much smaller diameter (Figure 6A, bottom right panel). This pH-responsive
14 mechanism for visualization is beneficial because high energy light sources can cause cell damage under
15 prolonged exposure. A movie of the chitosan coat shrinking upon increasing the pH is provided in the
16 supplementary materials (**Supplementary Movie 2**). To correlate the size of the capsules with the solution
17 pH, we incubated a population of chitosan encapsulated cells at increasing pH from 6 to 8 and imaged them
18 using fluorescence microscopy. We found a clear decrease and narrowing of the size distribution from ~ 80
19 μm to $\sim 15 \mu\text{m}$ upon increased the pH from 6 to 8. Collapse of the gel at pH 8 is expected to alter the
20 elasticity and porosity of the gel. We expect the ability to finely control physical features of the artificial
21 capsules can be relevant for different biochemical separation processes and controlled release of proteins
22 from the cells in many biotechnological and medical applications.

35 **Conclusions**

36
37
38 Cell encapsulation systems are by now well established. Typically single-cell encapsulation systems
39 rely on addition of initiating species from the external media. The novelty of the approach reported here is
40 based on three aspects. Firstly, the initiating enzyme is synthesized by the cell itself and displayed on the cell
41 wall, a process that originates from a plasmid-derived copy of the gene encoding the initiating GOx enzyme.
42 This means that the presence of the hydrogel capsule qualifies as an artificial cell phenotype, providing a
43 novel genotype-phenotype linkage. Secondly, the hydrogel shells reported here are robust and confer
44 significantly altered physical properties to the cells that make them easily processable in bulk operations. We
45 demonstrated isolation of the encapsulated cells using size-based filtration as well as immunity to enzymatic
46 and osmotic lysis mixtures. And thirdly, chitosan has been used as a tissue engineering scaffold but was this
47 far not utilized for enzyme-mediated single-cell encapsulation. The pH-responsiveness of chitosan capsules
48 can provide pH-tunable cell phenotypes.

49
50
51 Our system as described is compatible with yeast cells with ease of genetic manipulation and protein
52 display, however it is also generalizable to other cell types. Such an approach of displaying initiating
53 enzymes on the cell surface to initiate cell encapsulation reactions could be readily adapted to *E. coli* or
54
55
56
57
58
59
60

1
2
3 mammalian cell display systems in the future. Such a system is also adaptable to other classes of bio-
4 initiators, proteins and enzymes that can trigger radical polymerization providing a valuable tool for
5 visualization, protection and isolation of genetically high value cells from heterogeneous cell populations.
6 This new artificial eukaryotic cellular phenotype provides advantages for cell selection or evolution
7 campaigns and points towards the development of synthetic extracellular matrices or artificial biofilms that
8 can be programmed at the genetic level. This exciting area of bottom-up cell-directed materials synthesis is
9 one of the areas where we expect our presented reaction system to find significant applications.
10
11
12
13
14
15
16

17 **Acknowledgments**

18
19
20 We thank Ivan Urosev for help with ¹H-NMR measurements and data analysis. We thank Fabian
21 Rudolf and Florian Seebeck for helpful discussions. We are grateful to Martin Oeggerli (Micronaut) for
22 assistance with SEM imaging. We thank Nico Strohmeyer and Daniel Müller for assistance with further
23 imaging experiments. This work was funded by a Human Frontier Science Program (HFSP) Young
24 Investigator Grant (RGY80/2015), by Society in Science - The Branco Weiss Fellowship (ETH Zurich), and
25 by the National Center for Competence in Research Molecular Systems Engineering (NCCR-MSE).
26
27
28
29
30
31

32 **Supporting Information**

33
34
35 Supporting Figures (S1-S9) available. S1: ¹H-NMR spectrum of macromonomers; S2: GOx amplex red
36 assay on cell surface; S3: ABTS top agar assay; S4: 3D confocal fluorescence image of encapsulated cell;
37 S5: Additional fluorescence microscopy imaging of cells; S6: Flow cytometry plots of non-encapsulated vs.
38 encapsulated cells; S7: Trapping of extracellular fluorescent protein inside gel; S8: Growth curve of
39 encapsulated cells.
40
41
42
43
44
45

46 **Figure Captions**

47
48
49 *Scheme 1. Modification of macromonomers with phenols and fluorophores. (A) Reaction scheme for*
50 *production of alginate macromonomer. (B) Reaction scheme for preparation of chitosan macromonomer.*

51
52
53 *Figure 1. Overview of genetically encoded hydrogel encapsulation system for single cells. Scheme*
54 *depicting gene induction and yeast display of GOx homodimer, followed by enzyme-mediated cross-linking*
55 *of phenolated fluorescent monomers into a conformal hydrogel surrounding the cell. Modified monomers*
56 *carry fluorescein and phenol moieties are depicted as a green circle and yellow star, respectively.*
57
58
59
60

1
2
3 **Figure 2. Flow cytometry analysis of cells displaying GOx and enzymatically encapsulated in fluorescent**
4 **hydrogel.** (A) Flow cytometry analysis of (i) a yeast population displaying GOx and stained with anti-Xpress
5 antibody; (ii) yeast enzymatically encapsulated in fluorescent alginate hydrogel; and (iii) doubly stained
6 yeast population confirming surface display of GOx (Alexa fluor 555-labelled anti-Xpress antibody) and
7 encapsulation in fluorescent hydrogel (fluorescein-modified alginate). (B) Cell reference mixtures used to
8 test the fidelity of the encapsulation process. Decreasing amounts of GOx positive cells in the starting
9 mixtures were detected through analytical flow cytometry following the encapsulation reaction. An example
10 of a flow cytometry plot with the gate used for the analysis is shown on the right.

11
12
13
14
15
16 **Figure 3. Fluorescence imaging and sizing of alginate capsules.** (A) Confocal fluorescence microscopy
17 images of yeast cells individually encapsulated in a conformal alginate shell following 10 minute reaction.
18 Fluorescein incorporated in alginate capsules allowed direct visualization of the hydrogel shells in X, Y, and
19 Z projections using confocal fluorescence microscopy. (B) Hydrogel particle diameters (including cell
20 diameter) were measured at different reaction times ($n=10$ cells for each time point) by analyzing confocal
21 fluorescence images.

22
23
24
25
26 **Figure 4.** (A) SEM micrograph showing an encapsulated budding yeast adjacent to an unencapsulated
27 budding yeast cell. (B) SEM image of singly encapsulated yeast cells. Shell diameters are smaller under
28 vacuum SEM imaging conditions.

29
30
31
32 **Figure 5. Strategies for pGAL-GOx genotype enrichment.** (A) Immunity to enzymatic lysis. Genetically
33 heterogeneous yeast cell populations containing 10% cells carrying the pGAL-GOx gene were encapsulated
34 in fluorescent alginate and treated with lytic enzymes. The fraction of pGAL-GOx genotype-positive colonies
35 was quantified before and after enzymatic lysis. The recultivated population contained only pGAL-GOx
36 positive cells which were protected from enzymatic lysis by the hydrogel layer. (B) Size exclusion by
37 filtration. Encapsulated yeast cells in fluorescent alginate (green) were retained by the polycarbonate filter
38 with 10 μm pores (dark spots). Scale bar indicates 100 μm . (C) A yeast cell population containing 10% cells
39 carrying the pGAL-GOx gene was encapsulated in alginate and processed by filtration through a 10 μm pore
40 filter membrane. The majority of non-encapsulated cells was removed, resulting in 95% pGAL-GOx positive
41 cells retained on the filter.

42
43
44
45
46
47
48
49 **Figure 6. pH-responsive chitosan capsules.** (A, top) Single budding yeast cell encapsulated in a fluorescent
50 chitosan capsule at pH 6. The chitosan hydrogel is swollen and invisible in bright field. (A, bottom) Single
51 budding yeast cell encapsulated in fluorescent chitosan at pH 8. The polymer shell is collapsed around the
52 cell. At pH 8, the chitosan layer around the cells is also visible in bright field mode as indicated by the red
53 arrows. Scale bars indicate 10 μm . (B) Size distribution of chitosan-encapsulated single cells following
54 resuspension in aqueous buffers with increasing pH from 6 to 8. Average capsules diameters and standard
55 deviations: $67.6 \pm 20.5 \mu\text{m}$ at pH 6, $27.8 \pm 12.8 \mu\text{m}$ at pH 7, and $13.2 \pm 4 \mu\text{m}$ at pH 8 ($n>25$ cells for each
56 pH).

References

- (1) Wörsdörfer, B.; Woycechowsky, K. J.; Hilvert, D. Directed Evolution of a Protein Container. *Science* **2011**, *331*, 589–592.
- (2) Fischlechner, M.; Schaerli, Y.; Mohamed, M. F.; Patil, S.; Abell, C.; Hollfelder, F. Evolution of Enzyme Catalysts Caged in Biomimetic Gel-Shell Beads. *Nat. Chem.* **2014**, *6*, 791–796.
- (3) Sjostrom, S. L.; Bai, Y.; Huang, M.; Liu, Z.; Nielsen, J.; Joensson, H. N.; Andersson Svahn, H. High-Throughput Screening for Industrial Enzyme Production Hosts by Droplet Microfluidics. *Lab Chip* **2014**, *14*, 806–813.
- (4) Tawfik, D. S.; Griffiths, A. D. Man-Made Cell-like Compartments for Molecular Evolution. *Nat. Biotechnol.* **1998**, *16*, 652–656.
- (5) Mao, A. S.; Shin, J.-W.; Utech, S.; Wang, H.; Uzun, O.; Li, W.; Cooper, M.; Hu, Y.; Zhang, L.; Weitz, D. A.; et al. Deterministic Encapsulation of Single Cells in Thin Tunable Microgels for Niche Modelling and Therapeutic Delivery. *Nat. Mater.* **2017**, *16*, 236–243.
- (6) Theberge, A. B.; Courtois, F.; Schaerli, Y.; Fischlechner, M.; Abell, C.; Hollfelder, F.; Huck, W. T. S. Microdroplets in Microfluidics: An Evolving Platform for Discoveries in Chemistry and Biology. *Angew. Chem. Int. Ed Engl.* **2010**, *49*, 5846–5868.
- (7) Niu, J.; Lunn, D. J.; Pusuluri, A.; Yoo, J. I.; O'Malley, M. A.; Mitragotri, S.; Soh, H. T.; Hawker, C. J. Engineering Live Cell Surfaces with Functional Polymers via Cytocompatible Controlled Radical Polymerization. *Nat. Chem.* **2017**, *9*, 537–545.
- (8) Romero, G.; Lilly, J. J.; Abraham, N. S.; Shin, H. Y.; Balasubramaniam, V.; Izumi, T.; Berron, B. J. Protective Polymer Coatings for High-Throughput, High-Purity Cellular Isolation. *ACS Appl. Mater. Interfaces* **2015**, *7*, 17598–17602.
- (9) Shubin, A. D.; Felong, T. J.; Schutrum, B. E.; Joe, D. S. L.; Ovitt, C. E.; Benoit, D. S. W. Encapsulation of Primary Salivary Gland Cells in Enzymatically Degradable Poly(ethylene Glycol) Hydrogels Promotes Acinar Cell Characteristics. *Acta Biomater.* **2017**, *50*, 437–449.
- (10) Cahall, C. F.; Lilly, J. L.; Hirschowitz, E. A.; Berron, B. J. A Quantitative Perspective on Surface Marker Selection for the Isolation of Functional Tumor Cells. *Breast Cancer* **2015**, 1–11.
- (11) Karoubi, G.; Ormiston, M. L.; Stewart, D. J.; Courtman, D. W. Single-Cell Hydrogel Encapsulation for Enhanced Survival of Human Marrow Stromal Cells. *Biomaterials* **2009**, *30*, 5445–5455.
- (12) Lim, F.; Sun, A. M. Microencapsulated Islets as Bioartificial Endocrine Pancreas. *Science* **1980**, *210*, 908–910.
- (13) Uludag, H.; De Vos, P.; Tresco, P. A. Technology of Mammalian Cell Encapsulation. *Adv. Drug Deliv. Rev.* **2000**, *42*, 29–64.
- (14) Shoichet, M. S.; Li, R. H.; White, M. L.; Winn, S. R. Stability of Hydrogels Used in Cell Encapsulation: An in Vitro Comparison of Alginate and Agarose. *Biotechnol. Bioeng.* **1996**, *50*, 374–381.
- (15) Wu, P.-J.; Lilly, J. L.; Arreaza, R.; Berron, B. J. Hydrogel Patches on Live Cells through Surface-Mediated Polymerization. *Langmuir* **2017**, *33*, 6778–6784.
- (16) Lilly, J. L.; Berron, B. J. The Role of Surface Receptor Density in Surface-Initiated Polymerizations for Cancer Cell Isolation. *Langmuir* **2016**, *32*, 5681–5689.
- (17) Avens, H. J.; Berron, B. J.; May, A. M.; Voigt, K. R.; Sedorf, G. J.; Balasubramaniam, V.; Bowman, C. N. Sensitive Immunofluorescent Staining of Cells via Generation of Fluorescent Nanoscale Polymer Films in Response to Biorecognition. *J. Histochem. Cytochem.* **2011**, *59*, 76–87.
- (18) Sakai, S.; Taya, M. On-Cell Surface Cross-Linking of Polymer Molecules by Horseradish Peroxidase Anchored to Cell Membrane for Individual Cell Encapsulation in Hydrogel Sheath. *ACS Macro Lett.* **2014**, *3*, 972–975.
- (19) Yang, J.; Li, J.; Wang, X.; Li, X.; Kawazoe, N.; Chen, G. Single Mammalian Cell Encapsulation by in Situ Polymerization. *J. Mater. Chem. B Mater. Biol. Med.* **2016**, *4*, 7662–7668.
- (20) Kim, J. Y.; Lee, B. S.; Choi, J.; Kim, B. J.; Choi, J. Y.; Kang, S. M.; Yang, S. H.; Choi, I. S. Cytocompatible Polymer Grafting from Individual Living Cells by Atom-Transfer Radical

1
2
3
4
5
6
7
8
9
10
11
12
13
14
15
16
17
18
19
20
21
22
23
24
25
26
27
28
29
30
31
32
33
34
35
36
37
38
39
40
41
42
43
44
45
46
47
48
49
50
51
52
53
54
55
56
57
58
59
60

- Polymerization. *Angew. Chem. Int. Ed Engl.* **2016**, *55*, 15306–15309.
- (21) Rossi, N. A. A.; Constantinescu, I.; Brooks, D. E.; Scott, M. D.; Kizhakkedathu, J. N. Enhanced Cell Surface Polymer Grafting in Concentrated and Nonreactive Aqueous Polymer Solutions. *J. Am. Chem. Soc.* **2010**, *132*, 3423–3430.
- (22) Nguyen, K. T.; West, J. L. Photopolymerizable Hydrogels for Tissue Engineering Applications. *Biomaterials* **2002**, *23*, 4307–4314.
- (23) Malinowska, K. H.; Nash, M. A. Enzyme- and Affinity Biomolecule-Mediated Polymerization Systems for Biological Signal Amplification and Cell Screening. *Curr. Opin. Biotechnol.* **2016**, *39*, 68–75.
- (24) Kobayashi, S.; Uyama, H.; Kimura, S. Enzymatic Polymerization. *Chem. Rev.* **2001**, *101*, 3793–3818.
- (25) Shoda, S.-I.; Uyama, H.; Kadokawa, J.-I.; Kimura, S.; Kobayashi, S. Enzymes as Green Catalysts for Precision Macromolecular Synthesis. *Chem. Rev.* **2016**, *116*, 2307–2413.
- (26) Sakai, S.; Komatani, K.; Taya, M. Glucose-Triggered Co-Enzymatic Hydrogelation of Aqueous Polymer Solutions. *RSC Adv.* **2012**, *2*, 1502–1507.
- (27) Nakahata, M.; Gantumur, E.; Furuno, K.; Sakai, S.; Taya, M. Versatility of Hydrogelation by Dual-Enzymatic Reactions with Oxidases and Peroxidase. *Biochem. Eng. J.* **2018**, *131*, 1–8.
- (28) Kim, B. J.; Park, T.; Moon, H. C.; Park, S.-Y.; Hong, D.; Ko, E. H.; Kim, J. Y.; Hong, J. W.; Han, S. W.; Kim, Y.-G.; et al. Cytoprotective Alginate/polydopamine Core/shell Microcapsules in Microbial Encapsulation. *Angew. Chem. Int. Ed Engl.* **2014**, *53*, 14443–14446.
- (29) Park, J. H.; Hong, D.; Lee, J.; Choi, I. S. Cell-in-Shell Hybrids: Chemical Nanoencapsulation of Individual Cells. *Acc. Chem. Res.* **2016**, *49*, 792–800.
- (30) Kim, B. J.; Cho, H.; Park, J. H.; Mano, J. F.; Choi, I. S. Strategic Advances in Formation of Cell-in-Shell Structures: From Syntheses to Applications. *Adv. Mater.* **2018**, *30*, e1706063.
- (31) Wang, B.; Liu, P.; Jiang, W.; Pan, H.; Xu, X.; Tang, R. Yeast Cells with an Artificial Mineral Shell: Protection and Modification of Living Cells by Biomimetic Mineralization. *Angew. Chem. Int. Ed Engl.* **2008**, *47*, 3560–3564.
- (32) Pitzler, C.; Wirtz, G.; Vojcic, L.; Hiltl, S.; Böker, A.; Martinez, R.; Schwaneberg, U. A Fluorescent Hydrogel-Based Flow Cytometry High-Throughput Screening Platform for Hydrolytic Enzymes. *Chem. Biol.* **2014**, *21*, 1733–1742.
- (33) Sakai, S.; Kawakami, K. Synthesis and Characterization of Both Ionically and Enzymatically Cross-Linkable Alginate. *Acta Biomater.* **2007**, *3*, 495–501.
- (34) Kieke, M. C.; Cho, B. K.; Boder, E. T.; Kranz, D. M.; Wittrup, K. D. Isolation of Anti-T Cell Receptor scFv Mutants by Yeast Surface Display. *Protein Eng.* **1997**, *10*, 1303–1310.
- (35) Gietz, R. D.; Woods, R. A. Transformation of Yeast by Lithium Acetate/single-Stranded Carrier DNA/polyethylene Glycol Method. *Methods Enzymol.* **2002**, *350*, 87–96.
- (36) Swoboda, B. E. P.; Massey, V. Purification and Properties of the Glucose Oxidase from *Aspergillus Niger*. *J. Biol. Chem.* **1965**, *240*, 2209–2215.
- (37) Malinowska, K. H.; Verdorfer, T.; Meinhold, A.; Milles, L. F.; Funk, V.; Gaub, H. E.; Nash, M. A. Redox-Initiated Hydrogel System for Detection and Real-Time Imaging of Cellulolytic Enzyme Activity. *ChemSusChem* **2014**, *7*, 2825–2831.
- (38) Malinowska, K. H.; Rind, T.; Verdorfer, T.; Gaub, H. E.; Nash, M. A. Quantifying Synergy, Thermostability, and Targeting of Cellulolytic Enzymes and Cellulosomes with Polymerization-Based Amplification. *Anal. Chem.* **2015**, *87*, 7133–7140.
- (39) Zavada, S. R.; Battsengel, T.; Scott, T. F. Radical-Mediated Enzymatic Polymerizations. *Int. J. Mol. Sci.* **2016**, *17*, 195.
- (40) Uyama, H.; Kurioka, H.; Kobayashi, S. Novel Bienenzymatic Catalysis System for Oxidative Polymerization of Phenols. *Polym. J.* **1997**, *29*, 190–192.
- (41) Sigg, S. J.; Seidi, F.; Renggli, K.; Silva, T. B.; Kali, G.; Bruns, N. Horseradish Peroxidase as a Catalyst for Atom Transfer Radical Polymerization. *Macromol. Rapid Commun.* **2011**, *32*, 1710–1715.
- (42) Sakai, S.; Tsumura, M.; Inoue, M.; Koga, Y.; Fukano, K.; Taya, M. Polyvinyl Alcohol-Based Hydrogel Dressing Gellable on-Wound via a Co-Enzymatic Reaction Triggered by Glucose in the Wound Exudate. *J. Mater. Chem. B Mater. Biol. Med.* **2013**, *1*, 5067–5075.
- (43) Liu, Y.; Sakai, S.; Kawa, S.; Taya, M. Identification of Hydrogen Peroxide-Secreting Cells by Cytocompatible Coating with a Hydrogel Membrane. *Anal. Chem.* **2014**, *86*, 11592–11598.
- (44) Jin, R.; Moreira Teixeira, L. S.; Dijkstra, P. J.; Karperien, M.; van Blitterswijk, C. A.; Zhong, Z. Y.; Feijen, J. Injectable Chitosan-Based Hydrogels for Cartilage Tissue Engineering. *Biomaterials* **2009**, *30*, 2544–2551.

- 1
2
3 (45) de Campos, A. M.; Diebold, Y.; Carvalho, E. L. S.; Sánchez, A.; Alonso, M. J. Chitosan Nanoparticles
4 as New Ocular Drug Delivery Systems: In Vitro Stability, in Vivo Fate, and Cellular Toxicity. *Pharm.*
5 *Res.* **2004**, *21*, 803–810.
- 6 (46) Wang, H.; Lang, Q.; Li, L.; Liang, B.; Tang, X.; Kong, L.; Mascini, M.; Liu, A. Yeast Surface
7 Displaying Glucose Oxidase as Whole-Cell Biocatalyst: Construction, Characterization, and Its
8 Electrochemical Glucose Sensing Application. *Anal. Chem.* **2013**, *85*, 6107–6112.
- 9 (47) Pryor, W. A. Oxy-Radicals and Related Species: Their Formation, Lifetimes, and Reactions. *Annu. Rev.*
10 *Physiol.* **1986**, *48*, 657–667.
- 11 (48) Bernkop-Schnürch, A.; Dünnhaupt, S. Chitosan-Based Drug Delivery Systems. *Eur. J. Pharm.*
12 *Biopharm.* **2012**, *81*, 463–469.
- 13 (49) Szymańska, E.; Winnicka, K. Stability of Chitosan-a Challenge for Pharmaceutical and Biomedical
14 Applications. *Mar. Drugs* **2015**, *13*, 1819–1846.
- 15 (50) Imai, T.; Ohno, T. The Relationship between Viability and Intracellular pH in the Yeast *Saccharomyces*
16 *Cerevisiae*. *Appl. Environ. Microbiol.* **1995**, *61*, 3604–3608.
- 17
18
19
20
21
22
23
24
25
26
27
28
29
30
31
32
33
34
35
36
37
38
39
40
41
42
43
44
45
46
47
48
49
50
51
52
53
54
55
56
57
58
59
60

TOC Graphic

Cytoprotective genotype-phenotype linkage

